THE JOURNAL OF BIOLOGICAL CHEMISTRY VOL. 286, NO. 49, pp. 41917–41923, December 9, 2011

Molecular Determinants of $Ca_V2.1$ Channel Regulation by Calcium-binding Protein-1*[S]

Received for publication, August 10, 2011, and in revised form, September 26, 2011 Published, JBC Papers in Press, September 30, 2011, DOI 10.1074/jbc.M111.292417

Alexandra P. Few[1], **Evanthia Nanou**[1], **Todd Scheuer, and William A. Catterall**[2]

From the Department of Pharmacology, School of Medicine, University of Washington, Seattle, Washington 98195-7280

Background: Regulation of calcium channels by calcium-sensor proteins mediates short term synaptic plasticity.
Results: Calcium-binding protein-1 (CaBP1) inhibits calcium channels through its N terminus and second EF-hand, which is inactive in calcium binding.
Conclusion: Specific domains of CaBP1 are responsible for differential regulation, including an EF-hand inactive in calcium binding.
Significance: These results reveal the molecular code used by calcium-sensor proteins to differentially regulate short term synaptic plasticity.

Presynaptic $Ca_V2.1$ channels, which conduct P/Q-type Ca^{2+} currents, initiate synaptic transmission at most synapses in the central nervous system. Regulation of $Ca_V2.1$ channels by CaM contributes significantly to short term facilitation and rapid depression of synaptic transmission. Short term synaptic plasticity is diverse in form and function at different synapses, yet CaM is ubiquitously expressed. Differential regulation of $Ca_V2.1$ channels by CaM-like Ca^{2+} sensor (CaS) proteins differentially affects short term synaptic facilitation and rapid synaptic depression in transfected sympathetic neuron synapses. Here, we define the molecular determinants for differential regulation of $Ca_V2.1$ channels by the CaS protein calcium-binding protein-1 (CaBP1) by analysis of chimeras in which the unique structural domains of CaBP1 are inserted into CaM. Our results show that the N-terminal domain, including its myristoylation site, and the second EF-hand, which is inactive in Ca^{2+} binding, are the key molecular determinants of differential regulation of $Ca_V2.1$ channels by CaBP1. These findings give insight into the molecular code by which CaS proteins differentially regulate $Ca_V2.1$ channel function and provide diversity of form and function of short term synaptic plasticity.

P/Q-type Ca^{2+} currents conducted by $Ca_V2.1$ channels initiate synaptic transmission at most conventional fast synapses in the central nervous system (1, 2). Short term synaptic facilitation and rapid synaptic depression, on the time scale of milliseconds, strongly influence the response of synapses to trains of incoming action potentials (3, 4). Typically, synaptic transmission is strengthened by short trains of action potentials through synaptic facilitation, whereas long trains of action potentials cause depression of synaptic transmission. At the Calyx of Held, which is a large synapse in the auditory system, simultaneous recordings of presynaptic P/Q-type Ca^{2+} current and postsynaptic responses have shown that short term synaptic facilitation requires expression of $Ca_V2.1$ channels (5). Moreover, both short term facilitation and the rapid component of depression of synaptic transmission are correlated with the amplitude and kinetics of Ca^{2+}-dependent facilitation and inactivation of the P/Q-type Ca^{2+} current (6–9). These results implicate regulation of $Ca_V2.1$ channels in short term synaptic plasticity at the specialized Calyx of Held synapse, where both Ca^{2+} currents and synaptic transmission can be recorded simultaneously.

$Ca_V2.1$ channels expressed in nonneuronal cells are regulated by Ca^{2+}-dependent facilitation and inactivation (10, 11). These Ca^{2+}-dependent regulatory processes require interaction with Ca^{2+}/CaM (10, 11), which binds to a bipartite regulatory site in the C-terminal domain of these channels (10, 12, 13). Ca^{2+}-dependent facilitation is engaged by local increases in intracellular Ca^{2+}, whereas Ca^{2+}-dependent inactivation requires more sustained, global increases in intracellular Ca^{2+} (11). Ca^{2+}-dependent facilitation is mediated by high affinity Ca^{2+} binding to the C-terminal EF-hand of CaM, which interacts preferentially with an IQ-like motif in the C-terminal domain of $Ca_V2.1$ channels (12, 13). Ca^{2+}-dependent inactivation is mediated by lower affinity Ca^{2+} binding to the N-terminal EF-hands of CaM and subsequent interaction of the N-terminal domain of CaM (12) with a CaM binding domain (CBD)[3] located just downstream of the IQ-like motif in the C-terminal domain of $Ca_V2.1$ channels (10, 13). Mutations of the IQ-like motif and deletion of the CBD (ΔCBD) inhibit Ca^{2+}-dependent facilitation and inactivation, respectively (13). In sympathetic neurons, synaptic transmission driven by transfected $Ca_V2.1$ channels shows facilitation followed by depression in trains of stimuli, and facilitation and depression are inhibited by mutation of the IQ-like domain and the CBD, respectively (14). These results show that regulation of presynaptic Ca^{2+} chan-

* This work was supported, in whole or in part, by National Institutes of Health Grant R01 NS22625 (to W. A. C.) and Predoctoral Fellowship F31 MH078345 (to A. P. F.). This work was also supported by Swedish Research Council Postdoctoral Fellowship 524-2010-913 (to E. N.).
[S] The on-line version of this article (available at http://www.jbc.org) contains supplemental Tables 1 and 2.
[1] Both authors are co-first authors.
[2] To whom correspondence should be addressed. E-mail: wcatt@uw.edu.

[3] The abbreviations used are: CBD, CaM binding domain; ΔCBD, deletion of the CBD; CaBP1, Ca^{2+}-binding protein-1; CaS, CaM-like neuronal Ca^{2+} sensor; EGFP, enhanced GFP; VILIP-2, visinin-like protein-2.

nels by Ca^{2+}-dependent binding of CaM contributes substantially to short term synaptic plasticity (15).

Short term synaptic plasticity at different synapses is diverse in form and function (3, 4), suggesting that Ca^{2+} channel regulators in addition to ubiquitiously expressed CaM may be involved. The family of CaM-like neuronal Ca^{2+} sensor (CaS) proteins includes many members that are differentially expressed in different types of neurons and differentially regulate many neuronal functions (16–19), including Ca^{2+} currents and short term synaptic plasticity (20–23). Ca^{2+}-binding protein-1 (CaBP1), a neuron-specific CaS protein, interacts with $Ca_V2.1$ channels and modulates their activity in a manner distinct from CaM (20). Interaction of CaBP1 with the CBD positively shifts the voltage dependence of activation of $Ca_V2.1$ channels, supports faster inactivation in both single depolarizations and trains of depolarizations, and reduces Ca^{2+}-dependent facilitation (20). Sympathetic neuron synapses expressing $Ca_V2.1$ channels and CaBP1 have reduced synaptic facilitation and more rapid depression.[4] The experiments described here define the molecular basis for the differential regulation of $Ca_V2.1$ channels by the CaS protein CaBP1 and provide insight into the molecular code used by CaS proteins in differential regulation of short term synaptic plasticity.

EXPERIMENTAL PROCEDURES

Construction of Chimeras—All of the chimeras were named with a combination of two letters and four numbers. The letters are N for the N-terminal domain including the myristoyl moiety and H for the interlobe α-helix. The four numbers correspond to the four EF-hands from N to C terminus. The CaBP1 functional domains are highlighted in bold and underlined, whereas the CaM domains are in normal font. The ***N*12H34** chimera was generated by subcloning the N terminus of the long splice variant of CaBP1 (amino acids 1–80) into pcDNA3.1 and inserting it in-frame with CaM in pcDNA3.1. Similarly, the chimera ***N1*2H34** was generated by fusing the N terminus and EF-1 of CaBP1 (amino acids 1–183) in-frame with EF-hand 2, H, EF-hand 3, and EF-hand 4 of CaM (amino acids 46–end). The (***N12*H34**) chimera composed of the N terminus of CaBP1 (amino acids 1–80) fused to EF-hand 1 of CaM (amino acids 1–45), EF-hand 2 of CaBP1 (amino acids 120–150), and the central helix, EF-hand 3 and EF-hand 4 of CaM (amino acids 84-end) was generated using the ***N*12H34** chimera and replacing EF-2 of CaM (amino acids 46–83) with EF-2 of CaBP1 that was subcloned separately. The chimera ***N*12H*34*** was generated from ***N*12H34** by replacing EF-hand 3 and EF-hand 4 of CaM in with the corresponding EF-hand 3 and EF-hand 4 of CaBP1 (amino acids 160–227).

Cell Culture and Transfection—Prior to transfection, tsA-201 cells were grown to ~70% confluence in DMEM/Ham's F12 with 10% FBS (Atlanta Biologicals, Lawrenceville, GA) and 100 units/ml penicillin and streptomycin at 37 °C in 10% CO_2. Cells in 35-mm dishes were transfected with Ca^{2+} channel subunits α_{1A} (2 or 1.2 μg), β_{2a} (1.5 or 1 μg), $\alpha_2\delta$ (1 μg) with or without the long splice variant of CaBP1 (16), or a chimera (1 μg), using the Ca^{2+} phosphate method or FuGENE 6. CD8 (0.3 μg) was included to identify cells transfected with transmembrane proteins, and EGFP expression was used to select cells expressing chimeras or CaBP1. Throughout the results CaM indicates endogenous CaM present in tsA-201 cells. Throughout the results expression of $Ca_V2.1$ channels will indicate co-transfection of α_{1a}, β_{2a}, and $\alpha_2\delta$.

Electrophysiological Recording and Data Analysis—Whole cell voltage clamp recordings were obtained at room temperature 2–3 days after transfection. tsA-201 cells were incubated in extracellular solution containing 10 mM $CaCl_2$ or 10 mM $BaCl_2$, 150 mM Tris, 1 mM $MgCl_2$, and CD8 beads (Dynal, Oslo, Norway) to allow visualization of transfected cells. The intracellular solution consisted of 120 mM *N*-methyl-D-glucamine, 60 mM HEPES, 1 mM $MgCl_2$, 2 mM Mg-ATP, and 0.5 mM EGTA. The pH of intracellular and extracellular solutions was adjusted to 7.3 with methanesulfonic acid. Recordings were made using an HEKA EPC 9 patch clamp amplifier (HEKA Electronik, Lambrecht, Germany) with PULSE software (HEKA Elektronik) and filtered at 5 kHz. Leak and capacitive transients were subtracted using a P/-4 protocol. Because extracellular Ba^{2+} causes shifts in the voltage dependence of activation of −10 mV, voltage protocols were adjusted to compensate for this difference. Data analysis was performed using IGOR (Wavemetrics, Lake Oswego, OR). Individual traces of the data in Figs. 2, *A* and *B*, and 4, *A* and *B*, were smoothed prior to measuring I_{200} using a binomial algorithm smoothing within 20 points. Activation curves from each cell were fit to determine values for the voltage of half-activation ($V_{1/2}$) and the slope (k) using the Boltzmann equation: $y = (y_{max} - y_{min})/(1 + \exp(V_{1/2} - V)/k) + y_{min}$. All averaged data represent the mean ± S.E. Statistical significance was determined using one-way ANOVA.

RESULTS

Structure and Function of CaS Proteins—CaM and CaS proteins contain four EF-hand motifs separated into two pairs by a central α-helix (Fig. 1*A*). All four EF-hands in CaM are active in Ca^{2+} binding, whereas at least one of the two N-terminal EF-hands of the neuronal CaS proteins has molecular changes that prevent high affinity Ca^{2+} binding (Fig. 1*A*) (17, 18). In addition, the CaS proteins have an extended N-terminal domain with an N-terminal myristoyl lipid anchor. These molecular differences in the CaS proteins must be responsible for the differential regulation of $Ca_V2.1$ channels, yet the molecular determinants of this differential regulation are unknown. We constructed chimeric CaS proteins in which the regulatory domains of CaBP1 were progressively transferred into CaM (Fig. 1*A*) and analyzed their functional properties. Our strategy was to convert the regulatory properties of CaM to those of CaBP1, overexpress the chimeras to displace endogenous CaM, and detect the change of functional properties of the chimeras by their distinctive regulatory properties compared with endogenous CaM. Overexpression of CaM itself does not have any functional effects on $Ca_V2.1$ channels, suggesting that it is already at a saturating concentration (20). Therefore, distinctive regulatory effects conferred by expression of chimeras can be ascribed to the molecular changes in the chimeras themselves and not to additive effects of endogenous CaM plus the chimera. All of the chimeras we constructed were functionally

[4] K. Leal, S. Mochida, T. Scheuer, and W. A. Catterall, submitted.

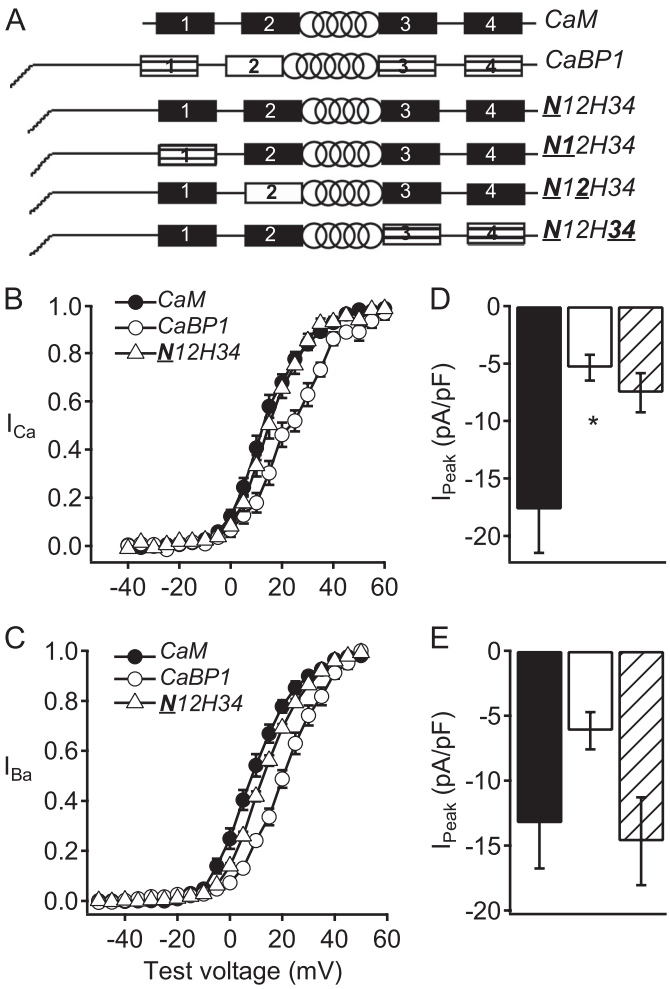

FIGURE 1. **Activation curves and peak currents of $Ca_V2.1$ channels modulated by chimera *N12H34*.** *A*, schematic of CaM/CaBP1 chimeras. EF-hands are indicated by *rectangles* and the central α helix is indicated by a *spiral*. *Filled rectangles*, CaM EF-hands; *striped rectangles*, CaBP1 EF-hands that bind Ca^{2+} with high affinity; *open rectangles*, CaBP1 EF-hands that do not bind Ca^{2+} with high affinity. *B* and *C*, normalized tail current-voltage curves were obtained by depolarizing from a holding potential of −80 mV to a variety of potentials and then repolarizing to −40 mV to elicit a tail current before returning to the holding potential (*B*) in Ca^{2+} for CaM (*filled circles*; $n = 16$), CaBP1 (*open circles*; $n = 7$), and ***N12H34*** chimera (*open triangles*; $n = 10$) and (*C*) in Ba^{2+} for CaM (*filled circles*; $n = 8$), CaBP1 (*open circles*; $n = 6$), and ***N12H34*** chimera (*open triangles*; $n = 10$). *D* and *E*, the peak inward current in the presence of Ca^{2+} (*D*) or Ba^{2+} (*E*) from the current-voltage curve was normalized to the capacitance estimated by integrating a 10-ms test pulse from −80 mV to −90 mV for CaM (*black*), CaBP1 (*white*), and ***N12H34*** chimera (*diagonal lines*). The data shown are averages ± S.E. (*error bars*). *Asterisk* indicates a significant difference from CaM (*, $p < 0.05$).

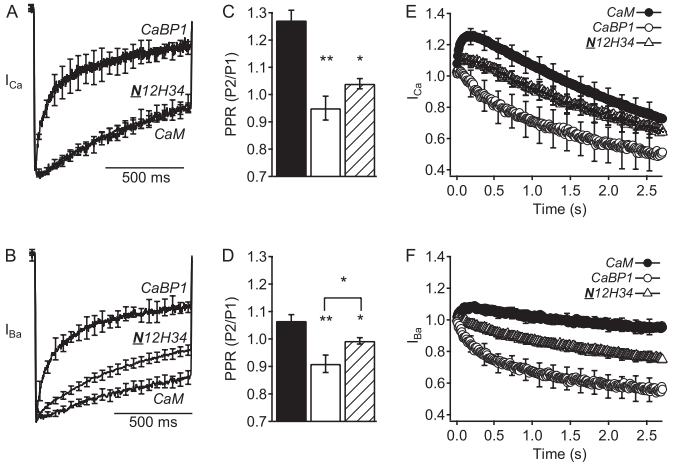

FIGURE 2. **Inactivation and facilitation of $Ca_V2.1$ channels modulated by chimera *N12H34*.** *A* and *B*, mean normalized currents elicited by a 1-s depolarization from −80 mV to (*A*) +30 mV in Ca^{2+} for CaM ($n = 13$), CaBP1 ($n = 10$), and ***N12H34*** chimera ($n = 8$) or (*B*) +20 mV in Ba^{2+} for CaM ($n = 6$), CaBP1 ($n = 6$), and ***N12H34*** chimera ($n = 14$). *C* and *D*, paired-pulse ratios (*PPR*) of CaM (*black*), CaBP1 (white), and ***N12H34*** chimera (*diagonal lines*) from tail currents evoked by test pulses 1.05 s before (*P1*) or 8 ms after (*P2*) a 50-ms depolarization to +10 mV to allow Ca^{2+} entry. Test pulses were from −80 mV to (*C*) +30 mV for Ca^{2+} currents or (*D*) +20 mV for Ba^{2+} currents followed by repolarization to −40 mV to evoke a tail current. *E* and *F*, normalized currents from repetitive depolarizations at a frequency of 100 Hz for 5 ms from −80 mV to (*E*) +20 mV in Ca^{2+} for CaM (*filled circles*; $n = 13$), CaBP1 (*open circles*; $n = 10$), and ***N12H34*** chimera (*open triangles*; $n = 8$) or (*F*) +10 mV in Ba^{2+} for CaM (*filled circles*; $n = 5$), CaBP1 (*open circles*; $n = 10$), and ***N12H34*** chimera (*open triangles*; $n = 8$). The data are averages ± S.E. (*error bars*). *Asterisks* indicate a significant difference from CaM over *error bars* or CaBP1 over *brackets* (**, $p < 0.01$; *, $p < 0.05$).

expressed because each of them had a clearly detectable effect on regulation of $Ca_V2.1$ channels (supplemental Tables 1 and 2). However, only one chimera was able to fully confer the regulatory properties of CaBP1 on CaM as described below.

Functional Effects of Transfer of the N-terminal Domain of CaBP1 to CaM—Previous studies showed that expression of CaBP1 causes reduced peak current, more positive voltage dependence of activation, more rapid inactivation in single depolarizations as well as in trains of depolarizations, and reduced facilitation in trains of depolarizations compared with endogenous CaM for $Ca_V2.1$ channels expressed in the human embryonic kidney cell line tsA-201 (20). To determine the molecular basis for these differences in Ca^{2+} channel regulation, we transferred functional domains of CaBP1 into CaM progressively, constructing CaBP1/CaM chimeras. Previous studies showed that deletion of the myristoylation site from the N terminus of CaBP1 prevented its differential regulation of $Ca_V2.1$ channels (24). A chimera in which the entire N-terminal domain of CaBP1 was substituted in CaM (***N12H34***) induced relatively negative voltage dependence of activation of both I_{Ca} and I_{Ba} similar to $Ca_V2.1$ channels in the presence of endogenous CaM (Fig. 1, *B* and *C*). However, this chimera showed reduced I_{Ca} like CaBP1 but not reduced I_{Ba} (Fig. 1, *D* and *E*).

Transfer of the N-terminal domain of CaBP1 into CaM in the ***N12H34*** chimera did not increase the rate of Ca^{2+}-dependent inactivation of I_{Ca} compared with that observed with endogenous CaM (Fig. 2*A*) and only partially increased the rate of inactivation of I_{Ba} toward the faster rate observed with CaBP1 (Fig. 2*B*). Nevertheless, this chimera significantly reduced both paired-pulse facilitation (Fig. 2, *C* and *D*) and facilitation in trains (Fig. 2, *E* and *F*), but not as effectively as CaBP1. Altogether, this chimera increased CaBP1-like regulation of inactivation of I_{Ba} during single depolarizations and significantly reduced facilitation during paired pulses and trains of depolarizations, but it was ineffective in transferring positively shifted voltage dependence of activation to CaM (Table 1).

Functional Effects of Transfer of EF-hand 1 of CaBP1 to CaM—To examine whether addition of EF-hand 1 of CaBP1 would transfer the functional properties of CaBP1 modulation of $Ca_V2.1$ channels, we constructed a chimera in which both the N-terminal domain and EF-hand 1 of CaBP1 were substituted in CaM (***N1*2H34**). The ***N1*2H34** chimera induced negative

voltage dependence of activation of both I_{Ca} and I_{Ba} and high peak current density similar to CaM (Fig. 3, *A* and *B*). In addition, this chimera induced inactivation of I_{Ca} and I_{Ba} that was similar to CaM and was slower than CaBP1 (Fig. 4, *A* and *B*). The ***N1*2H34** chimera induced paired-pulse facilitation that was similar to CaM, whereas facilitation in trains was significantly reduced compared with CaM, but not to the level observed with CaBP1 (Fig. 4, *E* and *F*). Taken together, these results suggest that the N terminus plus the EF-hand 1 of CaBP1 give some CaBP1-like effects when substituted in CaM, but are not sufficient for the positive voltage dependence of activation, enhanced inactivation, large reduction in facilitation, and decrease in the current density that are characteristic of CaBP1 modulation of $Ca_V2.1$ channels (Table 1).

Functional Effects of Transfer of EF-hand 2 of CaBP1 to CaM—A striking difference between the neuronal CaS proteins and CaM is the presence of an EF-hand motif in which amino acid substitutions prevent high affinity Ca^{2+} binding (16–19). Although these EF-hand motifs are inactive in Ca^{2+} binding, they may participate in Ca^{2+}-independent regulatory interactions. Consistent with an important functional role for the inactive EF-hand 2, binding of CaBP1 to $Ca_V2.1$ channels does not require Ca^{2+}, and the effects of CaBP1 on the voltage dependence of activation, peak current amplitude, time course of inactivation, and facilitation in trains of depolarizations are all observed for Ba^{2+} currents recorded in the absence of Ca^{2+} (20). To test the functional role of EF-hand 2 of CaBP1, we constructed an additional chimera in which both the N-terminal domain and the second EF-hand motif of CaBP1 were transferred into CaM (***N12*H34**) (Fig. 1*A*). This chimera shifted the activation of $Ca_V2.1$ channels to more positive voltages, like $Ca_V2.1$ channels regulated by CaBP1 (Fig. 5, *A* and *B*) and reduced peak $Ca_V2.1$ channel currents like CaBP1 (Fig. 5, *C* and *D*). Moreover, this chimera increased the rate of inactivation of both I_{Ca} and I_{Ba} as effectively as CaBP1 (Fig. 6, *A* and *B*). The ***N12*H34** chimera also reduced paired-pulse facilitation like CaBP1 (Fig. 6, *C* and *D*) and prevented facilitation of both I_{Ca} and I_{Ba} in trains of depolarizations similarly to CaBP1 (Fig. 6, *E*

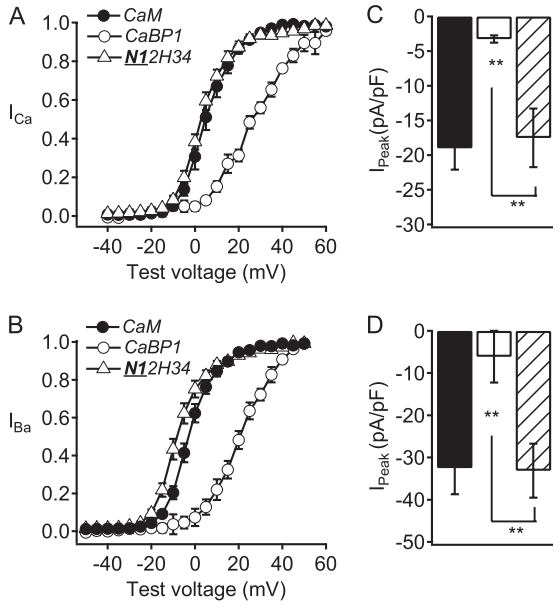

FIGURE 3. **Activation curves and peak currents of $Ca_V2.1$ channels modulated by chimera *N12H34*.** *A* and *B*, normalized tail current-voltage curves were obtained by depolarizing from a holding potential of −80 mV to a variety of potentials and then repolarizing to −40 mV to elicit a tail current before returning to the holding potential (*A*) in Ca^{2+} for CaM (*filled circles*; $n = 13$), CaBP1 (*open circles*; $n = 8$), and ***N1*2H34** chimera (*open triangles*; $n = 10$) and (*B*) in Ba^{2+} for CaM (*filled circles*; $n = 10$), CaBP1 (*open circles*; $n = 8$), and ***N1*2H34** chimera (*open triangles*; $n = 10$). *C* and *D*, the peak inward current from the current-voltage curve was normalized to the capacitance estimated by integrating a 10-ms test pulse from −80 mV to −90 mV for CaM (*black*), CaBP1 (*white*), and ***N1*2H34** chimera (*diagonal lines*). The data shown are averages ± S.E. (*error bars*). *Asterisks* indicate a significant difference from CaM over *error bars* or CaBP1 over *brackets* (**, $p < 0.01$).

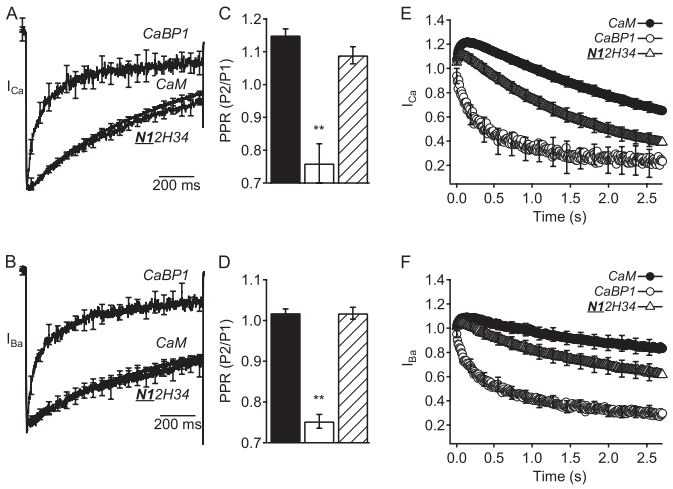

FIGURE 4. **Inactivation and facilitation of $Ca_V2.1$ channels modulated by chimera *N12H34*.** *A* and *B*, normalized currents elicited by a 1-s depolarization from −80 mV to (*A*) +30 mV in Ca^{2+} for CaM ($n = 10$), CaBP1 ($n = 8$), and ***N1*2H34** chimera ($n = 8$) or (*B*) +20 mV in Ba^{2+} for CaM ($n = 6$), CaBP1 ($n = 8$), and ***N1*2H34** chimera ($n = 10$). *C* and *D*, paired-pulse ratios (*PPR*) of CaM (*black*), CaBP1 (*white*), and ***N1*2H34** chimera (*diagonal lines*) from tail currents evoked by test pulses 1.05 s before (*P1*) or 8 ms after (*P2*) a 50-ms depolarization to +10 mV to allow Ca^{2+} entry. Test pulses were from −80 mV to (*C*) +30 mV for Ca^{2+} currents or (*D*) +20 mV for Ba^{2+} currents followed by repolarization to −40 mV to evoke a tail current. *E* and *F*, normalized currents from repetitive depolarizations at a frequency of 100 Hz for 5 ms from −80 mV to (*E*) +20 mV in Ca^{2+} for CaM (*filled circles*; $n = 13$), CaBP1 (*open circles*; $n = 10$), and ***N1*2H34** chimera (*open triangles*; $n = 15$) or (*F*) +10 mV in Ba^{2+} for CaM (*filled circles*; $n = 10$), CaBP1 (*open circles*; $n = 10$), and ***N1*2H34** chimera (*open triangles*; $n = 8$). The data are averages ± S.E. (*error bars*). *Asterisks* indicate a significant difference from CaM (**, $p < 0.01$).

TABLE 1

Summary of functional effects of CaBP1/CaM chimeras

The transfer of regulatory properties of CaBP1 to CaM is indicated by the symbols: −, regulatory property of CaM is retained; +, regulatory property of CaBP1 is effectively transferred in the chimera; ±, regulatory property of CaBP1 is partially transferred in the chimera.

Construct	$V_{1/2}$	Peak current	Rate of inactivation	Paired-pulse facilitation	Facilitation in trains
CaM	−	−	−	−	−
N12H34	−	+	−	±	±
N12H34	−	−	−	−	±
N12H34	+	+	+	+	+
N12H34	−	−	−	±	±
CaBP1	+	+	+	+	+

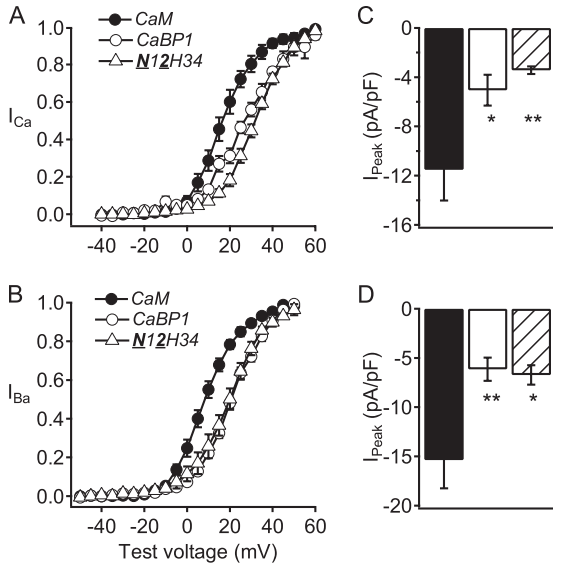

FIGURE 5. **Activation curves and peak currents of $Ca_V2.1$ channels modulated by chimera *N12H34*.** Normalized tail current-voltage curves were obtained by depolarizing from a holding potential of −80 mV to a variety of potentials and then repolarizing to −40 mV to elicit a tail current before returning to the holding potential (*A*) in Ca^{2+} for CaM (*filled circles*; $n = 6$), CaBP1 (*open circles*; $n = 5$), and ***N12H34*** chimera (*open triangles*; $n = 10$) and (*B*) in Ba^{2+} for CaM (*filled circles*; $n = 9$), CaBP1 (*open circles*; $n = 10$), and ***N12H34*** chimera (*open triangles*; $n = 9$). *C* and *D*, the peak inward current from the current-voltage curve was normalized to the capacitance estimated by integrating a 10-ms test pulse from −80 mV to −90 mV for CaM (*black*), CaBP1 (*white*), and ***N12H34*** chimera (*diagonal lines*). The data shown are averages ± S.E. (*error bars*). *Asterisks* indicate a significant difference from CaM (*, $p <$ 0.05; **, $p < 0.01$).

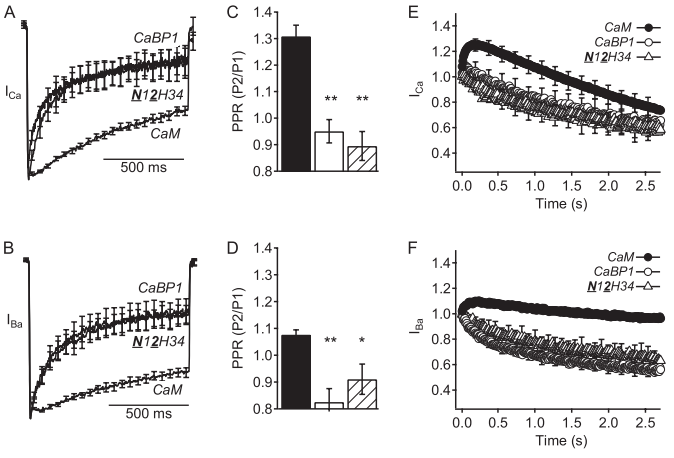

FIGURE 6. **Inactivation and facilitation of $Ca_V2.1$ channels modulated by chimera *N12H34*.** *A* and *B*, normalized currents elicited by a 1-s depolarization from −80 mV to (*A*) +30 mV in Ca^{2+} for CaM ($n = 10$), CaBP1 ($n =$ 8), and ***N12H34*** chimera ($n = 8$) or (*B*) +20 mV in Ba^{2+} for CaM ($n = 6$), CaBP1 ($n = 8$), and ***N12H34*** chimera ($n = 10$). *C* and *D*, paired-pulse ratios (*PPR*) of CaM (*black*), CaBP1 (*white*), and ***N12H34*** chimera (*diagonal lines*) from tail currents evoked by test pulses 1.05 s before (*P1*) or 8 ms after (*P2*) a 50-ms depolarization to +10 mV to allow Ca^{2+} entry. Test pulses were from −80 mV to (*C*) +30 mV for Ca^{2+} currents or (*D*) +20 mV for Ba^{2+} currents followed by repolarization to −40 mV to evoke a tail current. *E* and *F*, normalized currents from repetitive depolarizations at a frequency of 100 Hz for 5 ms from −80 mV to (*E*) +20 mV in Ca^{2+} for CaM (*filled circles*; $n = 13$), CaBP1 (*open circles*; $n = 10$), and ***N12H34*** chimera (*open triangles*; $n = 15$) or (*F*) +10 mV in Ba^{2+} for CaM (*filled circles*; $n = 10$), CaBP1 (*open circles*; $n = 10$), and ***N12H34*** chimera (*open triangles*; $n = 8$). The data are averages ± S.E. (*error bars*). *Asterisks* indicate a significant difference from CaM (**, $p < 0.01$; *, $p < 0.05$).

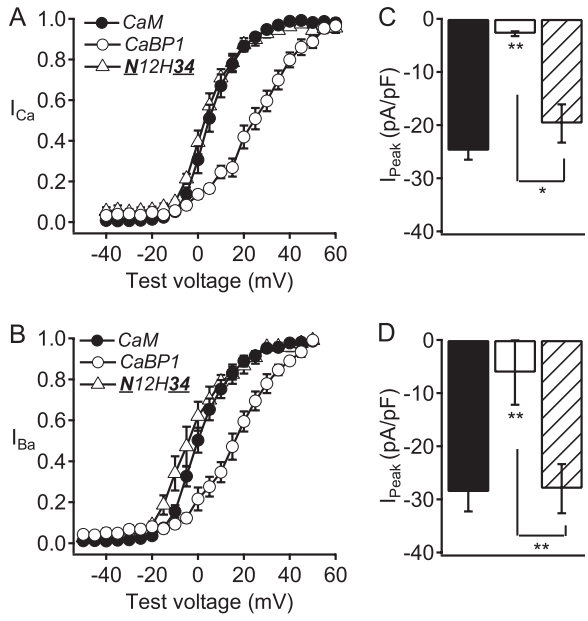

FIGURE 7. **Activation curves and peak currents of $Ca_V2.1$ channels modulated by chimera *N12H34*.** Normalized tail current-voltage curves were obtained by depolarizing from a holding potential of −80 mV to a variety of potentials and then repolarizing to −40 mV to elicit a tail current before returning to the holding potential (*A*) in Ca^{2+} for CaM (*filled circles*; $n = 6$), CaBP1 (*open circles*; $n = 5$), and ***N12H34*** chimera (*open triangles*; $n = 10$) and (*B*) in Ba^{2+} for CaM (*filled circles*; $n = 9$), CaBP1 (*open circles*; $n = 10$), and ***N12H34*** chimera (*open triangles*; $n = 9$). *C* and *D*, the peak inward current from the current-voltage curve was normalized to the capacitance estimated by integrating a 10-ms test pulse from −80 mV to −90 mV for CaM (*black*), CaBP1 (*white*), and ***N12H34*** chimera (*diagonal lines*). The data shown are averages ± S.E. (*error bars*). *Asterisks* indicate a significant difference from CaM over *error bars* or CaBP1 over *brackets* (**, $p < 0.01$; *, $p < 0.05$).

and F). Thus, all of the regulatory properties of CaBP1 were transferred to CaM in a chimera containing the N-terminal and EF-hand 2 of CaBP1 (Table 1).

Functional Effects of Transfer of the C-terminal Lobe of CaBP1 to CaM—Finally, we examined the functional role of the C-terminal lobe of CaBP1 together with its N terminus substituted in CaM (***N12H34***). Expression of $Ca_V2.1$ channels with the ***N12H34*** chimera gave negative voltage dependence of activation and normal peak current density for both I_{Ca} and I_{Ba} like $Ca_V2.1$ channels in the presence of endogenous CaM alone (Fig. 7). In addition, $Ca_V2.1$ channels expressed with the ***N12H34*** chimera had a slow rate of inactivation similar to expression with endogenous CaM and significantly different from CaBP1 (Fig. 8, *A* and *B*). However, compared with CaM, the ***N12H34*** chimera induced somewhat less paired-pulse facilitation in the presence of Ca^{2+} (Fig. 8*C*) and both reduced facilitation and increased inactivation of $Ca_V2.1$ channels during trains of depolarizations compared with CaM (Fig. 8, *E* and *F*). Overall, this chimera retained CaM-like voltage dependence of activation, high expression level, and regulation of inactivation of I_{Ca} and I_{Ba} during single depolarizations, and it gained partial CaBP1-like effects in reducing facilitation and enhancing inactivation during paired pulses and trains of depolarizations (Table 1).

DISCUSSION

Molecular Basis for Differential Regulation of $Ca_V2.1$ Channels by CaBP1—The neuron-specific CaS proteins differ from CaM in their N-terminal myristoylation, their extended N-ter-

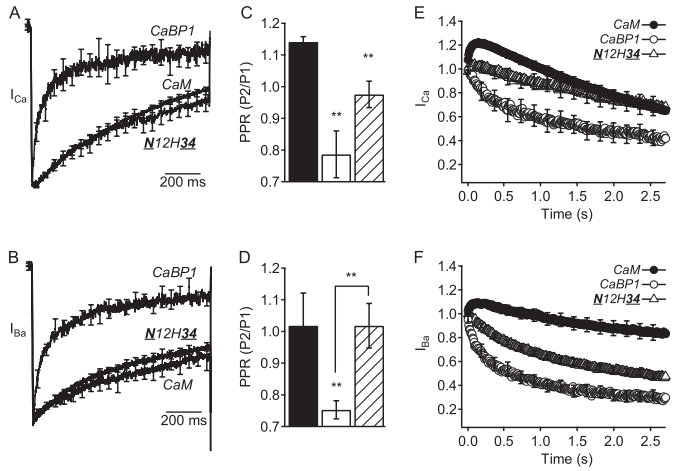

FIGURE 8. **Inactivation and facilitation of $Ca_V2.1$ channels modulated by chimera *N12H34*.** *A* and *B*, normalized currents elicited by a 1-s depolarization from −80 mV to (*A*) +30 mV in Ca^{2+} for CaM ($n = 10$), CaBP1 ($n = 8$), and ***N12H34*** chimera ($n = 8$) or (*B*) +20 mV in Ba^{2+} for CaM ($n = 6$), CaBP1 ($n = 8$), and ***N12H34*** chimera ($n = 10$). *C* and *D*, paired-pulse ratios (*PPR*) of CaM (*black*), CaBP1 (*white*), and ***N12H34*** chimera (*diagonal lines*) from tail currents evoked by test pulses 1.05 s before (*P1*) or 8 ms after (*P2*) a 50-ms depolarization to +10 mV to allow Ca^{2+} entry. Test pulses were from −80 mV to (*C*) +30 mV for Ca^{2+} currents or (*D*) +20 mV for Ba^{2+} currents followed by repolarization to −40 mV to evoke a tail current. *E* and *F*, normalized currents from repetitive depolarizations at a frequency of 100 Hz for 5 ms from −80 mV to (*E*) +20 mV in Ca^{2+} for CaM (*filled circles*; $n = 13$), CaBP1 (*open circles*; $n = 10$), and ***N12H34*** chimera (*open triangles*; $n = 15$) or (*F*) +10 mV in Ba^{2+} for CaM (*filled circles*; $n = 10$), CaBP1 (*open circles*; $n = 10$), and ***N12H34*** chimera (*open triangles*; $n = 8$). The data are averages ± S.E. (*error bars*). *Asterisks* indicate a significant difference from CaM over *error bars* or CaBP1 over *brackets* (**, $p < 0.01$).

minal domains, and their EF-hands that are inactive in Ca^{2+} binding (16–19). Previous studies showed that myristoylation is required for differential regulation of $Ca_V2.1$ channels by CaBP1 and visinin-like protein-2 (VILIP-2) (23, 24). Our results presented here show that the differential regulation of $Ca_V2.1$ channels by CaBP1 and CaM are primarily determined by the N-terminal domain and the second EF-hand, which is inactive in Ca^{2+} binding (16–19). Transfer of these two domains into CaM fully confers CaBP1-like regulatory properties, including reduced peak current, positively shifted voltage dependence of activation, increased rate of inactivation, reduced paired-pulse facilitation, and reduced facilitation during trains of depolarizations (Table 1). In contrast, substitution of the N-terminal lobe or other EF-hands gave at most partial transfer of CaBP1 properties (Table 1). These results provide the initial insights into the molecular code used by CaS proteins in differential regulation of Ca^{2+} channel function. Evidently, molecular changes in specific domains of the CaS proteins are sufficient to confer these differential Ca^{2+} channel regulatory properties.

It is unexpected that EF-hand 2, which is predicted to be inactive in Ca^{2+} binding, is dominant among the four EF-hands in transferring the regulatory effects of CaBP1 to CaM. This EF-hand has two complementary effects. First, it displaces CaM as indicated by the loss of Ca^{2+}-dependent facilitation induced by CaM. Second, it induces more rapid, Ca^{2+}-independent inactivation than observed with CaM, which indicates that its binding causes Ca^{2+}-independent acceleration of inactivation. These results imply that EF-hand 2 is constitutively in an activated conformation with respect to these regulatory effects of CaBP1 on $Ca_V2.1$ channels. Because the neuronal CaS proteins all have at least one EF-hand that is predicted to be inactive in Ca^{2+} binding, it is possible that these inactive EF-hands also play a dominant regulatory role in other CaS protein-dependent regulatory processes.

In addition to the N-terminal and EF-hand 2, transfer of other EF-hands from CaBP1 to CaM gave partial CaBP1 effects, suggesting that these domains also contribute to the overall function of CaBP1 (Table 1). In particular, The ***N12H34*** chimera supported partial CaBP1-like effects to reduce facilitation and enhance inactivation of $Ca_V2.1$ channels during trains of stimuli (Table 1). These results show that substitution for the C-terminal lobe of CaM, which is responsible for Ca^{2+}-dependent facilitation (13), reduces facilitation partially even without transfer of EF-hand 2 of CaBP1. Thus, even though EF-hand 2 of CaBP1 is dominant in transferring its regulatory effects, perhaps because it is constitutively in an activated conformation in the absence of Ca^{2+}, other EF-hands of CaBP1 may further enhance its Ca^{2+}-dependent regulatory functions because they have partial effects when transferred into CaM by themselves (Table 1).

Ca^{2+} Sensor Proteins and Short Term Synaptic Plasticity—Within the family of CaS proteins, CaBP1 can displace CaM from their common interaction site on $Ca_V2.1$ channels and enhance inactivation (20), whereas VILIP-2 binds at the same site and enhances facilitation (23). CaBP1 and VILIP-2 differentially regulate synaptic plasticity when overexpressed at sympathetic neuron synapses expressing $Ca_V2.1$ channels.[4] These results show that the neuronal CaS proteins can bind to the same bipartite regulatory site as CaM on $Ca_V2.1$ channels but cause differential regulation of Ca^{2+} channel function and short term synaptic plasticity.

At the Calyx of Held, facilitation of P/Q-type Ca^{2+} currents contributes significantly to short term synaptic facilitation (5, 6), and Ca^{2+}-dependent inactivation of P/Q-type Ca^{2+} currents contributes significantly to the rapid phase of synaptic depression (7, 8). In transfected sympathetic neurons, regulation of $Ca_V2.1$ channels by CaM is required for short term synaptic facilitation and rapid synaptic depression at sympathetic neuron synapses transfected with wild-type and mutant $Ca_V2.1$ channels (14). These results all point to an important role for regulation of $Ca_V2.1$ channels by CaM and CaS proteins in short term synaptic plasticity.

The form of short term synaptic plasticity differs widely among synapses, with very different ratios of facilitation and depression (3, 4), but the molecular basis for the diversity of short term synaptic plasticity is unknown. CaM is ubiquitious and cannot effectively provide diversity of synaptic plasticity in different types of neurons and synapses. Our results presented here suggest that differential regulation of presynaptic Ca^{2+} channels by the "inactive" EF-hands of neurospecific CaS proteins may provide diversity of short term synaptic plasticity. Analysis of the molecular determinants of differential Ca^{2+} channel regulation by other members of the CaS family of proteins will provide further insight into the molecular code that these proteins use for differential modulation of short term synaptic plasticity.

Acknowledgments—We thank Elizabeth M. Sharp and Dr. Gilbert Martinez for excellent technical assistance in molecular biology.

REFERENCES

1. Llinás, R., Sugimori, M., Hillman, D. E., and Cherksey, B. (1992) *Trends Neurosci.* **15,** 351–355
2. Dunlap, K., Luebke, J. I., and Turner, T. J. (1995) *Trends Neurosci.* **18,** 89–98
3. Zucker, R. S., and Regehr, W. G. (2002) *Annu. Rev. Physiol.* **64,** 355–405
4. Abbott, L. F., and Regehr, W. G. (2004) *Nature* **431,** 796–803
5. Inchauspe, C. G., Martini, F. J., Forsythe, I. D., and Uchitel, O. D. (2004) *J. Neurosci.* **24,** 10379–10383
6. Cuttle, M. F., Tsujimoto, T., Forsythe, I. D., and Takahashi, T. (1998) *J. Physiol.* **512,** 723–729
7. Forsythe, I. D., Tsujimoto, T., Barnes-Davies, M., Cuttle, M. F., and Takahashi, T. (1998) *Neuron* **20,** 797–807
8. Xu, J., and Wu, L. G. (2005) *Neuron* **46,** 633–645
9. Xu, J., He, L., and Wu, L. G. (2007) *Curr. Opin. Neurobiol.* **17,** 352–359
10. Lee, A., Wong, S. T., Gallagher, D., Li, B., Storm, D. R., Scheuer, T., and Catterall, W. A. (1999) *Nature* **399,** 155–159
11. Lee, A., Scheuer, T., and Catterall, W. A. (2000) *J. Neurosci.* **20,** 6830–6838
12. DeMaria, C. D., Soong, T. W., Alseikhan, B. A., Alvania, R. S., and Yue, D. T. (2001) *Nature* **411,** 484–489
13. Lee, A., Zhou, H., Scheuer, T., and Catterall, W. A. (2003) *Proc. Natl. Acad. Sci. U.S.A.* **100,** 16059–16064
14. Mochida, S., Few, A. P., Scheuer, T., and Catterall, W. A. (2008) *Neuron* **57,** 210–216
15. Catterall, W. A., and Few, A. P. (2008) *Neuron* **59,** 882–901
16. Haeseleer, F., Sokal, I., Verlinde, C. L., Erdjument-Bromage, H., Tempst, P., Pronin, A. N., Benovic, J. L., Fariss, R. N., and Palczewski, K. (2000) *J. Biol. Chem.* **275,** 1247–1260
17. Haeseleer, F., and Palczewski, K. (2002) *Adv. Exp. Med. Biol.* **514,** 303–317
18. Burgoyne, R. D., and Weiss, J. L. (2001) *Biochem. J.* **353,** 1–12
19. Burgoyne, R. D., O'Callaghan, D. W., Hasdemir, B., Haynes, L. P., and Tepikin, A. V. (2004) *Trends Neurosci.* **27,** 203–209
20. Lee, A., Westenbroek, R. E., Haeseleer, F., Palczewski, K., Scheuer, T., and Catterall, W. A. (2002) *Nat. Neurosci.* **5,** 210–217
21. Tsujimoto, T., Jeromin, A., Saitoh, N., Roder, J. C., and Takahashi, T. (2002) *Science* **295,** 2276–2279
22. Sippy, T., Cruz-Martín, A., Jeromin, A., and Schweizer, F. E. (2003) *Nat. Neurosci.* **6,** 1031–1038
23. Lautermilch, N. J., Few, A. P., Scheuer, T., and Catterall, W. A. (2005) *J. Neurosci.* **25,** 7062–7070
24. Few, A. P., Lautermilch, N. J., Westenbroek, R. E., Scheuer, T., and Catterall, W. A. (2005) *J. Neurosci.* **25,** 7071–7080